Testing the Potential of GPR-FWI to Detect Tracer Plumes in Time-Lapse Monitoring

Peleg Haruzi [a,*], Nils Gueting [a], Anja Klotzsche [a,b], Jan Vanderborght [a,b], Harry Vereecken [a,b], Jan van der Kruk [a,b]

[a]Agrosphere Institute, IBG-3, Forschungszentrum Jülich GmbH
[b]Centre for High-Performance Scientific Computing in Terrestrial Systems (HPSC-TerrSys), Geoverbund ABC/J

SPONSORED BY

This study is part the Enigma ITN program (European training Network for in situ imaGing of dynaMic processes in heterogeneous subsurfAce environments). This project has received funding from the European Union's Horizon 2020 research and innovation programme under the Marie Sklodowska-Curie Grant Agreement No 722028.

Introduction

Transport processes can be monitored using geophysical methods when the tracer changes the geophysical properties of the aquifer (e.g. electrical conductivity, permittivity) and when these changes can be resolved in space and time. Time-lapse single-hole ground penetration radar (GPR) imaging of saline tracer in fractured rock demonstrated the potential to monitor transport processes (Shakas et al., 2017). Crosshole GPR measurements processed by the full-waveform inversion (FWI) method show models with significantly higher resolution and improved localization of fine-scale heterogeneity compared to their ray-based counterparts (Klotzsche et al., 2010). In the current research, a time-lapse crosshole GPR imaging of a saline tracer test is planned in an alluvial aquifer in Krauthausen test site (Kemna at al., 2002), to test the potential of GPR-FWI to detect transport processes. Hereby we present synthetic time-lapse GPR-FWI imaging of a saline tracer test.

Synthetic Tracer Test - Workflow

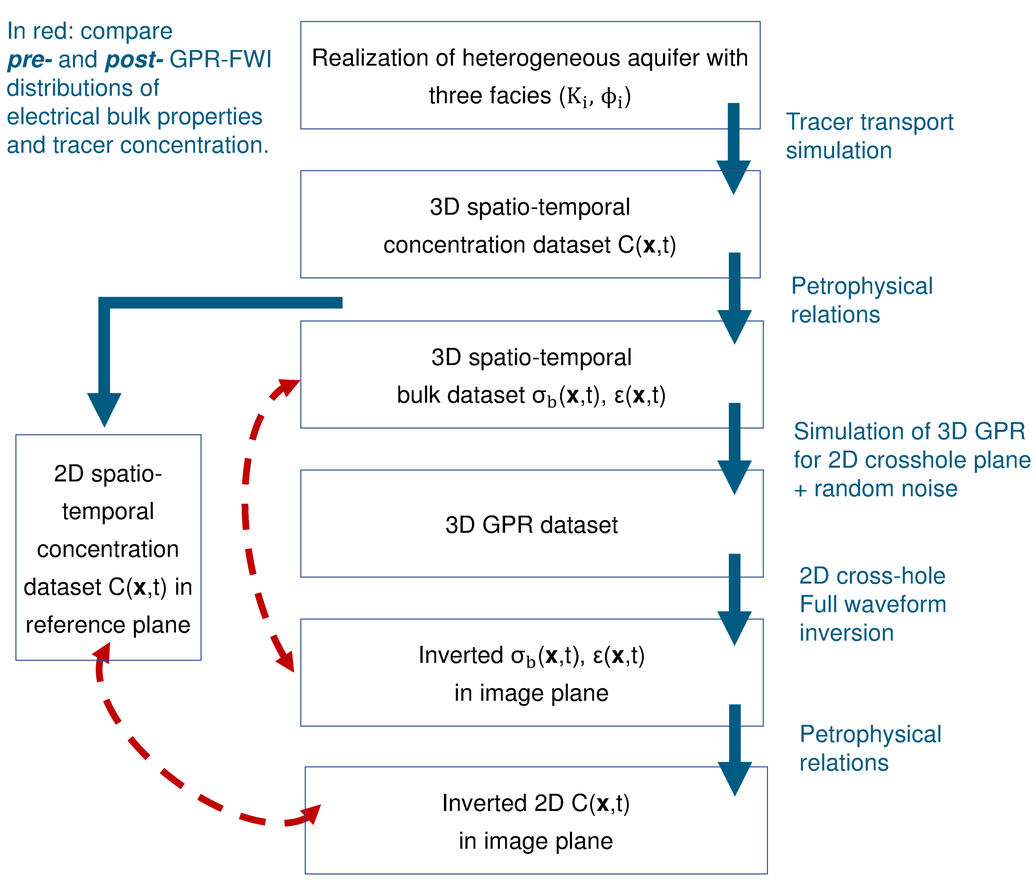

Petrophysical Relations

Bulk electrical conductivity (σ_b) is influenced by introducing electrolytes in the groundwater, whereas permittivity (ε) is not affected by it (Giannakis, 2016). The tracer concentration (C) was converted to bulk electrical conductivity by the following relations:

- The total groundwater salinity ($S_{GW,tot}$) was calculated as sum of the ambient salinity (0.398 g/kg) and the tracer salinity:

$$S_{GW,tot}(\mathbf{x},t) = S_{GW,ambient} + \frac{C(\mathbf{x},t)}{C_{injection}} \times S_{injection} \quad (1)$$

- The groundwater water conductivity (σ_{GW}) was related to salinity and temperature of the water using empirical relations (Stogryn, 1971):

$$\sigma_{GW}(\mathbf{x},t) = f(S_{GW}(\mathbf{x},t),T) \quad (2)$$

- The bulk conductivity was calculated from Archie's empirical law (Archie, 1942), using the formation factor (F), an intrinsic measure of material microgeometry:

$$\sigma_b(\mathbf{x},t) = \frac{\sigma_{GW}(\mathbf{x},t)}{F(\mathbf{x})} \quad (3)$$

$F(\mathbf{x},\mathbf{t}=0)$ was calculated in ambient conditions from GPR-FWI bulk conductivity $\sigma_b(\mathbf{x})$ (Figure 3b) and uniform groundwater conductivity σ_{GW}.

Tracer Transport Simulation

A 3D tracer transport was simulated through hydrogeological model (Fig. 1) of an alluvial aquifer in Krauthausen test site, composed of three facies (Table 1). Distribution of the tracer (Fig. 2) manifests a leading plume in the top gravel part of the aquifer, and a slower plume in the more sandy part at the bottom of the aquifer. Tracer concentration in crosshole plane was converted to electrical conductivity (Fig. 2e-g) using petrophysical relations (Eq. 1-3).

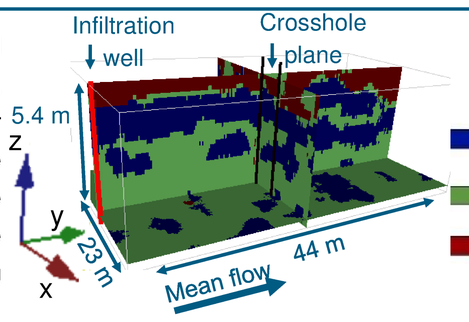

Figure 1: 3D hydrogeological model (modified from Gueting et al., 2018), based on GPR-FWI results and co-located grain size data (Gueting et al. 2015 and 2017). The model cell size is (0.18m)^3.

Facie	K $[m/day]$	ϕ	α_L $[m]$	α_T $[m]$
1: sand	14.3	0.29	0.1	0.01
2: sandy gravel	70.2	0.25	0.1	0.01
3: gravel	626	0.18	0.1	0.01

Table 1, Flow and transport parameters of the 3D model: hydraulic conductivity (K), porosity (ϕ), longitudinal (α_L) and transverse dispersivity (α_T).

Synthetic GPR Full-Waveform Inversion

GPR acquisition setup: Synthetic crosshole GPR forward model simulations (Ricker wavelet, $f_c = 120$ MHz) were performed in a multi-offset gather semi-reciprocal acquisition setup, with spatial sampling of 0.1 m and 0.2 m for the receivers and transmitters, respectively. The crosshole plane distance was 3.4m, located 20 m downstream from the injection borehole, perpendicular to the mean flow direction (Fig. 2d). Time-lapse GPR were simulated for the background (ambient conditions, t=0), and at selected tracer arrival time (t=20 days), when salinity and electrical conductivity were 30% higher than the counterpart ambient groundwater.

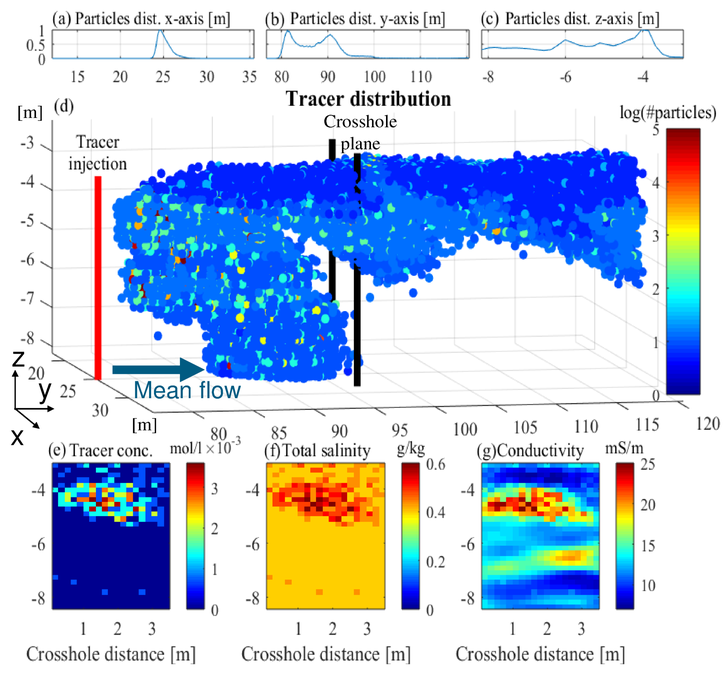

Figure 2: 3D transport simulation 20 days after injection and derived electrical conductivity plane for GPR simulation. (a-c) spatial distribution of the tracer across the 3 dimensions; (d) 3D spatial distribution of the particles; (e) tracer concentration in the crosshole plane (d); (f,g) total groundwater salinity and electrical conductivity calculated using petrophysical relations. (Flow and transport simulations were run on TRACE and PARTRACE codes, Vereecken et al and Bechtold et al., 2012). Figure adapted from Haruzi et al., 2018.

Full-waveform inversion setup: The real models (RM) of the background and tracer were taken from GPR-FWI field measurements (ε_r of both cases - Fig. 3a; σ_b background - Fig. 3b; Gueting et al., 2015) and from transport simulation (σ_b tracer - Fig. 2g). The starting models (SM) for ε_r for background and tracer were generated by smoothing the RM (Fig. 3c), where the SM for both σ_b cases were both a uniform mean of the σ_b background RM (Fig. 3d).

Time-lapse crosshole GPR-FWI: The background FWI (Fig. 4a.b) generated similar models to the real models (Fig. 3a,b). For the tracer case, whilst the ε_r FWI model (Fig. 4c) was similar to the RM, the σ_b model (Fig. 4d) generated an image which reconstructs successfully the tracer location (at 4.5m depth) but smooths the heterogeneity in σ_b at the cell-scale (0.09m), to a region of intermediate σ_b. Differences in time-lapse σ_b FWI models of tracer and background cases (Fig. 4f) resulted in a smoothed reconstruction of the plume (compare with Fig. 2e). The mean inverted salinity of the plume from FWI (0.16 g/kg) was similar to that of the transport simulation (0.12 g/kg). Differences of the ε_r FWI models were very low, as expected.

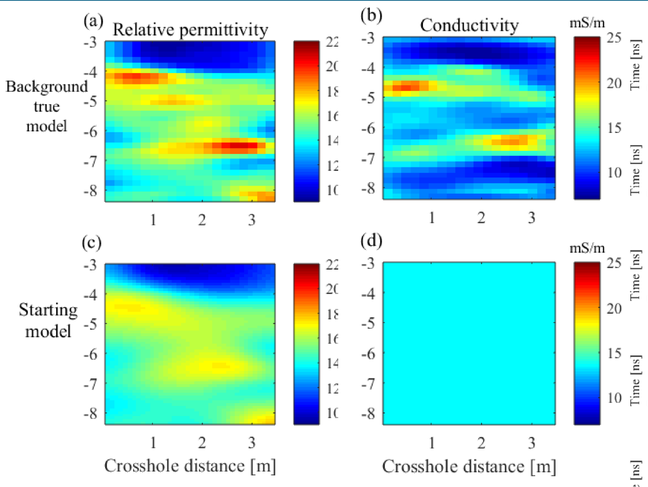

Figure 3: Relative permittivity and conductivity background true models (a, b) and starting models (c, d) for the FWI.

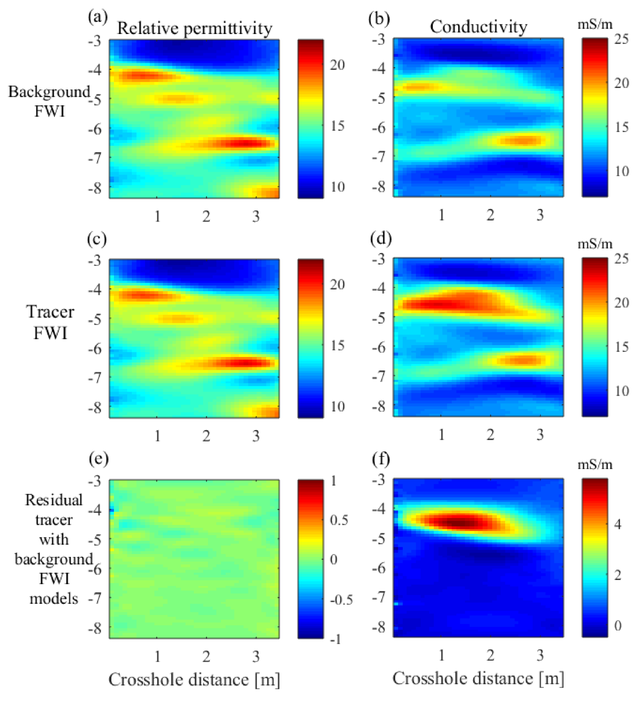

Figure 4: (a, b) FWI results of background model; (c, d) FWI results of tracer model data 20 days after injection; (e) Difference of permittivity models (c) and (a); (f) Difference of conductivity models (d) and (b).

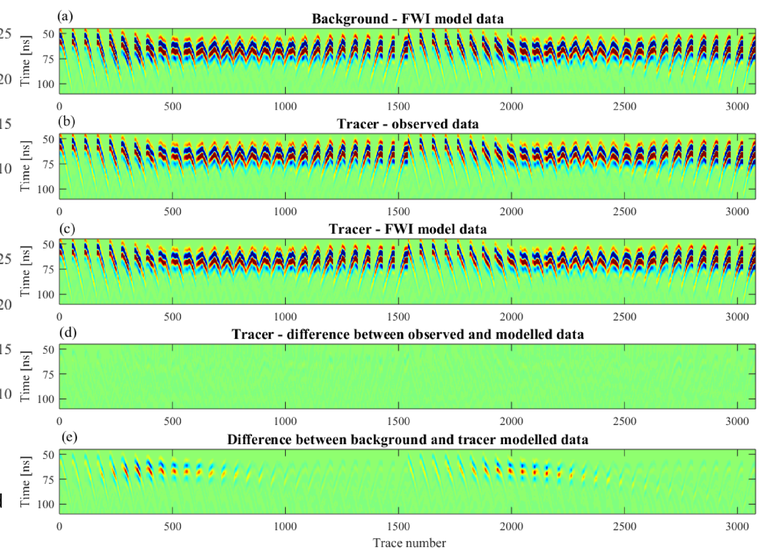

Figure 5: See titles above. The x-axis denotes trace number starting from the first trace of first transmitter gather and ending to last trace of last transmitter gather.

Time-lapse GPR-FWI - transmitter gathers: Comparison of transmitter gathers from observed and FWI modelled data of the tracer arrival scenario (Fig. 5b,c) resulted in small residuals (Fig. 5d), suggesting that the FWI converged successfully to the observed data. Comparison between transmitter gathers from background (Fig. 5a) and tracer modelled data (Fig. 5c) present large differences in amplitudes for transmitter gathers located at the upper part of the boreholes (traces 200-800 for transmitters at the left borehole, and traces 1700-2300 at the right borehole). The amplitude difference is due to signal attenuation in the tracer model, explained by the tracer plume that infiltrated through the upper part of the crosshole plane (Fig. 2d,e).

Conclusions and Outlook

- GPR-FWI detected infiltration of saline tracer at the decimeter scale, however it smoothed finer scale heterogeneities (compare Fig. 2e and Fig. 4f).
- Based on the prediction from transport simulation and the ability to detect the tracer in various concentrations, a field tracer is planned in Krauthausen test site.

For future work we plan:

- to test the full-waveform inversion for larger electrical conductivity contrasts, which were found to be a more challenging case for conversion to the real model.
- to use zero-offset (ZOP) crosshole acquisition to analyze whether using with quick method a tracer infiltration can be detected and on which conductivity contrasts.

References

Archie, 1942., Transactions of the AIME, 146(01), 54-62.
Bechtold et al., 2012. Vadose Zone Journal, 11(2).
Giannakis, 2016. PhD dissertation, The University of Edinburgh.
Gueting et al., 2015. Journal of hydrology, 524, 680-695.
Gueting et al., 2017. Water Resources Research, 53(1), 49-72.
Gueting et al., 2018. Mathematical Geosciences, 1-23.
Haruzi et al., 2018. *SEG Technical Program Expanded Abstracts*.
Kemna et al., *Journal of Hydrology*, *267*(3-4), 125-146.
Klotzsche et al., 2010. *Near surface geophysics*, 8(6), 635-649.
Shakas, et al., 2017. *Geophysical Research Letters*, *44*(8), 3663-3671.
Stogryn, 1971. *IEEE transactions on microwave theory and Techniques*, 19(8), 733-736.
Vereecken et al., 1994. ICG-4 (IBG-3) Int. Rep. 501494, Forschungszentrum Jülich.